Environmental Toxicology and Chemistry, 2025, 1–15
https://doi.org/10.1093/etojnl/vgaf213
Advance access publication: September 4, 2025
Original Article

Environmental Toxicology

Gene expression changes in ducklings exposed in ovo to emerging and legacy per-/poly-fluoroalkyl substances

Anne-Fleur Brand[1], Silje Peterson[1,2], Louisa M.S. Günzel[1], Kang Nian Yap[1], Tomasz M. Ciesielski[1,3], Céline Arzel[2], and Veerle L.B. Jaspers[1,*]

[1]Department of Biology, Norwegian University of Science and Technology (NTNU), Trondheim, Norway
[2]Department of Biology, University of Turku, Turku, Finland
[3]Department of Arctic Technology, The University Centre in Svalbard (UNIS), Longyearbyen, Norway

*Corresponding author: Veerle L.B. Jaspers. Email: veerle.jaspers@ntnu.no

Abstract

This study investigated the effects of two emerging per- and polyfluoroalkyl substances (PFAS), perfluorododecane sulfonic acid (PFDoDS) and perfluoro-4-ethylcyclohexane sulfonic acid (PFECHS), alongside legacy perfluorooctanesulfonic acid (PFOS) on mallard ducklings (*Anas platyrhynchos*) exposed in ovo. These PFAS compounds were selected based on their detection in a declining sea duck species and concerns over their endocrine disruption potential. Farmed mallard eggs were injected with 80 ng/g of PFDoDS, PFECHS, or PFOS, simulating maternal transfer to the egg and reflecting concentrations at the upper end of those reported in wild bird eggs. Gene expression was assessed in the liver, heart, and bursa of Fabricius. In the liver, messenger RNA (mRNA) and small RNA sequencing revealed sex-specific changes in genes related to metabolism and immune function, particularly antiviral responses, in PFECHS- and PFDoDS-exposed ducklings. Notably, there was overlap between male PFECHS- and PFOS-exposed groups. In the heart, quantitative polymerase chain reaction (qPCR) analyses of mRNAs and microRNAs associated with stress, inflammation, and development showed no differences, though trends included altered expression of genes involved in oxidative and cellular stress responses across treatments. In the bursa of Fabricius, qPCR of immune-related mRNAs revealed upward trends in innate immune gene expression across all exposure groups, also consistent with antiviral immune activation, suggesting shared transcriptional effects among these sulfonated PFAS. These findings demonstrate that emerging PFAS exposure alters gene regulation related to key physiological pathways, with responses differing by sex and tissue type. Our results underscore the complexity of PFAS-induced immunomodulation and highlight potential developmental risks of maternal PFAS transfer in wild avian species.

Keywords: per-/poly-fluoroalkyl substances, mallard, gene expression, immunomodulation, metabolism

Introduction

Global migratory waterfowl populations are declining under various pressures (Wetlands International, 2025), with the role of pollutant exposure remaining unclear. Among the myriad of pollutants, per- and polyfluoroalkyl substances (PFAS) represent a particularly concerning class. Per- and polyfluoroalkyl substances encompass a diverse group of thousands of man-made compounds that contain at least one aliphatic perfluorocarbon moiety (e.g., $-C_nF_{2n}-$; Kwiatkowski et al., 2020). While many studies have been performed on legacy PFAS, including perfluorooctanesulfonic acid (PFOS)—which is listed under the Stockholm Convention and has been linked to developmental toxicity, immunotoxicity, hepatotoxicity, and carcinogenicity (Antonopoulou et al., 2024)—much less is known about the impacts of emerging PFAS. Notably, recent findings suggest that some novel PFAS compounds may be more harmful than their legacy counterparts (Briels et al., 2018), highlighting the need for further research on their impacts as they enter the environment. The present study investigates the effects of two emerging PFAS compounds—perfluoro-4-ethylcyclohexane sulfonic acid (PFECHS or PFEtCHxS) and perfluorododecane sulfonic acid (PFDoDS or PFDoS)—on toxicity pathways in avian species, which have not been reported to date.

The cyclic eight-carbon PFECHS is used as an anticorrosive agent in aircraft hydraulic fluids (De Silva et al., 2011) and is frequently found around airports. It has been widely detected in environmental samples, including tissues from various bird species (Sun et al., 2023). Regarding its toxicity, mixed findings have been reported, depending on the organism, exposure levels, and context. Houde et al. (2013) found no relationships between vitellogenin (VTG) expression in the liver, VTG plasma activity, and PFECHS plasma concentrations (5.07 ± 4.72 ng/g wet wt) in environmentally exposed northern pike (*Esox lucius*), while they reported a VTG decrease in *Daphnia magna* (0.06 and 6 mg/L), suggesting endocrine disruptive potential (Houde et al., 2016). In marine *Chlorella* sp., chronic exposure to 1000 ng/L PFECHS reduced growth (Niu et al., 2019). In vivo exposure of zebrafish (*Danio rerio*) to PFECHS resulted in deformities and increased the expression of key genes (*PPARα*, *CYP1A1*, and *APOA1* at 0.5–2.5 μg/L; Mahoney et al., 2023a), altered pathways related to cellular interaction, focal adhesion, MAPK signaling, and actin cytoskeleton regulation (0.006–5 mg/L; Mahoney et al., 2024), and induced oxidative stress,

Received: June 3, 2025. **Revised:** August 12, 2025.

immunotoxicity, reduced heart rate, and impaired spontaneous movement (100 μg/L; Yao et al., 2024). Moreover, in vitro (*Oncorhynchus mykiss* liver cells), PFECHS disrupted mitochondrial membranes and gene expression, significantly affecting glutathione-S-transferase at 400 ng/L, while other genes were dysregulated only at non-environmentally relevant concentrations (Mahoney et al., 2023b). The same study reported PFECHS to induce reactive oxygen species (ROS) production in a dose-dependent manner at treatments of 0.2–180 mg/L. These findings suggest that PFECHS toxicity involves multiple pathways, including ROS induction, endocrine disruption, alterations in cellular signaling, and disruptions to membrane integrity and function. Of the studies comparing effects of PFECHS with PFOS, toxicity relative to PFOS varies depending on the biological endpoint assessed (Mahoney et al., 2023a, 2023b; Yao et al., 2024).

The 12-carbon PFDoDS is a newer compound, the specific uses of which are not well documented or widely reported. It has been detected in several Southern Ocean seabird species (Roscales et al., 2019) and was recently found in eggs from declining sea duck populations at concentrations exceeding those of legacy PFOS, raising concerns about developmental effects (Frøyland, 2022). To the author's knowledge, no studies have reported PFDoDS exposure effects to date.

The establishment of a clear link between PFAS exposure and their effects in situ is often hampered by unknown influences of additional factors such as environmental conditions, occurrence of co-contaminants, and age and sex of the investigated species. To overcome these challenges, we conducted a controlled laboratory study using the mallard (*Anas platyrhynchos*) as a model species for avian wildlife. In ovo injection, administered before the start of incubation, allows for the introduction of PFAS directly into the yolk sac, where these compounds are known to accumulate (Gebbink & Letcher, 2012). This exposure pathway mimics maternal transfer, providing a relevant model for studying developmental toxicity. By euthanizing the ducklings immediately after hatching, we can observe changes during a critical developmental window, offering insights into the potential early-life impacts of PFAS exposure.

Exposure to PFAS (with PFOS as a focal chemical in most studies) during development has been linked to effects in various organs in birds, including the liver, the heart, and the bursa of Fabricius (Briels et al., 2018; Geng et al., 2019; Mattsson et al., 2019). The liver is an important target organ for many types of PFAS and a main accumulation site (Robuck et al., 2021). Per- and polyfluoroalkyl substance exposure can lead to various adverse effects in the liver, including disruptions in metabolic processes (Geng et al., 2019). In the heart, exposure to PFAS has been shown to induce cardiotoxicity, including abnormal cardiac morphology and impaired heart function (Wen et al., 2023). These effects on the heart, observed in embryonic models, highlight the risks associated with PFAS exposure during early development. Lastly, the bursa of Fabricius is crucial for the avian immune system and can be affected by PFAS during critical stages of development (Mattsson et al., 2019).

The present study was designed to investigate the effects of PFDoDS and PFECHS, alongside PFOS, on gene expression in three key organs: the liver, heart, and bursa of Fabricius. To capture the full range of potential gene expression responses to PFAS exposure in the liver, a major target organ, we used RNA sequencing as a nontargeted approach, particularly because no information on molecular pathways is available for PFDoDS. In addition to messenger RNA (mRNA), microRNA (miRNA) expression was also assessed. MicroRNAs are small, noncoding RNA molecules of approximately 22 nucleotides in length. They regulate gene expression by binding to complementary sequences in mRNAs, leading to mRNA degradation or inhibition of translation (Bartel, 2004). This post-transcriptional regulation allows miRNAs to control the expression of a wide variety of genes involved in critical cellular processes, including growth, differentiation, immune responses, metabolism, and responses to chemical stressors. An increasing number of studies highlight the role of miRNAs in mediating responses to PFAS, including in the liver (Dong et al., 2016; Wang et al., 2015). In the heart, miRNA-490 has been implicated in PFAS-induced effects in chickens (*Gallus gallus*; Guo et al., 2022). More broadly, miRNA-21 plays a key role in cardiovascular disease (Krichevsky & Gabriely, 2009), while miRNAs 1 and 133 are crucial for heart development (Wystub et al., 2013). These miRNAs were therefore selected for targeted expression analysis in the heart to investigate their potential role in PFAS-induced cardiotoxicity, particularly in relation to reported changes in cardiac function and morphology in birds. Alongside miRNA analysis, genes related to the cellular stress response in the avian heart (Seremelis et al., 2019) were assessed to provide insight into specific molecular pathways contributing to PFAS-induced cardiotoxicity. Lastly, in the bursa of Fabricius, a subset of immune genes was targeted to assess the immunotoxic potential of PFDoDS and PFECHS in birds.

Our overall aim was to identify molecular pathways disrupted by developmental exposure to the emerging PFAS, PFDoDS, and PFECHS, alongside legacy PFOS, in three key tissues. We hypothesize that in ovo exposure to these compounds may lead to gene expression changes similar to those induced by PFOS. By integrating both mRNA and miRNA analysis, this combined approach provides a more comprehensive understanding of PFAS toxicity in avian species, enhancing our knowledge essential for effective environmental regulation and wildlife conservation efforts.

Methods

All experimental procedures involving animals were approved by the Norwegian Food Safety Authority (Mattilsynet; FOTS ID 30237) and carried out at the animal laboratory facilities of the Department of Biology at the Norwegian University of Science and Technology (NTNU) in Norway.

The in ovo study investigated a multitude of endpoints, including hatching success, time of developmental arrest in unhatched eggs, morphometrics, PFAS concentrations in duckling tissues, and plasma hormone concentrations in hatched ducklings. Results for these endpoints are presented in Peterson (2024).

Chemicals

Chemicals were purchased from Chiron (Trondheim, Norway). Perfluorooctane sulfonic acid (CAS No. 1763-23-1, net purity 94.6 ± 4.0%) and perfluoro-4-ethylcyclohexanesulfonic acid, potassium salt (PFECHS-K, CAS No. 335-24-0, net purity 94.3%) were supplied as powders, while PFDoDS (CAS No. 79780-39-5, net purity 98.9%) was purchased dissolved in methanol. Solvent-rinsed glassware and equipment were used during the preparation of the compounds and the delivery vehicle (see "Vehicle preparation" section) to minimize background contamination. For PFOS and PFECHS-K, solutions (500 μg/ml) were made by dissolving the compounds in sterilized ultrapure water (PURELAB Flex, Elga), followed by ultrasonication (Ultrasonic Cleaner USC-TH, VWR). For PFECHS, the concentration was adjusted to reflect the PFECHS anion, not the potassium salt.

Vehicle preparation

For in ovo administration of the compounds, an emulsion of lecithin and peanut oil in water was prepared, based on Brunström

and Örberg (1982) with minor modifications. Lecithin from egg yolk (GPR RECTAPUR; VWR Chemicals BDH, Leuven, Belgium) was dissolved in dichloromethane (EMSURE ACS; MilliporeSigma, Darmstadt, Germany) and mixed with peanut oil (Sigma-Aldrich, St Louis, MO, USA; lecithin: peanut oil, 1:10, w:v). Dichloromethane was evaporated at 38 °C under 200 mbar using a rotary evaporator (RV 10, IKA).

For each compound, an emulsion with a concentration of 40 ng/µl was prepared to achieve a final dose of 80 ng/g egg, reflecting concentrations at the upper end of those reported in eggs of wild birds, including common eiders (*Somateria mollissima*) from the Baltic Sea (Frøyland, 2022). An overview of reported PFDoDS, PFECHS, and PFOS concentrations in eggs from various bird species is presented in online supplementary material Table S1. The vehicle control emulsion was prepared by mixing three parts (4.8 ml) of sterile ultrapure water with two parts (3.2 ml) of lecithin/peanut oil mixture. For PFECHS and PFOS emulsions, the water-dissolved compounds (approximately 500 µg/ml) were diluted in sterile ultrapure water prior to the addition of the lecithin/peanut oil mixture (water:lecithin/peanut oil, 3:2, v:v) to obtain the desired final concentrations. For PFDoDS, 200 ng dissolved in methanol was added to the lecithin:peanut oil mixture (2.4 ml), followed by methanol evaporation at 39 °C under 200 mbar. Next, sterile ultrapure water (3.6 ml) was added to form an emulsion. All emulsions were autoclaved (25 min, 120 °C) and sonicated three times for 30 s using a probe (GEX 400 Laboratory Ultrasonic Processor with CV26 Probe, Cole Parmer) to promote mixing, dispersion, and emulsification. The final emulsions were stored at 4 °C prior to injection (within 1–3 days).

Egg injections

Fertilized mallard eggs were purchased from a breeding farm in Sweden (Scandinavian High-Flyers AB, Heberg). The eggs were collected on the day of oviposition and transported and stored at 10 °C–15 °C to maintain dormancy for 4–6 days post-laying. The eggs ($n = 149$) were randomly divided into exposure groups and one control group, and were injected over 3 consecutive days (Days 4, 5, or 6 post-laying) before incubation on Day 0. To minimize the number of animals in this study, we used only one control group (a vehicle-injected control group) based on previous in ovo experiments in our lab that compared non-injected, punctured, and vehicle-injected control groups (Briels et al., 2018). Prior to the experiment, 10 mallard eggs from the same breeding farm were incubated to assess the incubation setup in a pilot study; all ducklings hatched within 28 days.

To avoid thermal shock during incubation at 37.8 °C, the cooled eggs were brought up to room temperature before injection. The emulsions were also brought to room temperature and sonicated (Ultrasonic Processor GEX 400, Cole Parmer) prior to injection. Eggs were weighed (Precision Balance ME4002, Mettler Toledo) to determine the injection volume, followed by disinfection of the blunt end of the egg with 90% ethanol. The drilling, injecting, and sealing of eggs were carried out in a laminar flow hood (LaminAir PCR Mini, Holten). A rounded dentist drill bit mounted on a hand-held electric drill (Robust AC Rotary Tool Multitool) was used to create a 1 mm Ø hole while avoiding puncturing the inner shell membrane. Using a 250 µl gastight syringe (Model 1725 TLL, PTFE Luer Lock, Hamilton) and sterile needles (Sterican Ø 0.80 × 40 mm 21G × 1 1/2″, B.Braun), the emulsions were injected into the yolk sac of the egg. The injected volume ranged from 99 to 145 µl, depending on the egg mass (2 µl/g egg); egg mass ranged from 49.4 to 72.4 g (mean ± SD: 59.3 ± 4.5 g). Following injection, holes were sealed with paraffin.

Egg incubation

Injected eggs from the different groups were evenly distributed over three automatically turning incubators (HEKA 1+ and HEKA 3 Wooden Egg Incubators, HEKA, Verl, Germany) and kept at 37.8 °C. Relative humidity was maintained at approximately 55% by manual spraying. The development of the embryos was monitored using candling. Eggs that showed no development after 1 week of incubation or released a smell indicative of decomposition were frozen at −20 °C. These eggs, along with all unhatched eggs, were opened (and sampled if appropriate) at the end of the experiment to assess their developmental status. On incubation Day 25, eggs were transferred to hatching boxes, and humidity was increased to 65%–80%. Both the timing of pipping and hatching was recorded to calculate pipping and hatching success (percentage of fertile eggs that were able to pip externally and hatch, respectively).

Results on hatching and pipping success, embryonic development stages in unhatched eggs for both hatched and unhatched ducklings, and morphometrics (head size, tarsus, and ulna length) for pipped and hatched ducklings are presented in Peterson (2024).

Sampling

Hatched ducklings were removed from the hatching boxes as soon as they were dry (< 12 hr after hatching), weighed, and euthanized by decapitation with sharp scissors. The sex of the ducklings was determined by amplifying a region of the chromo-helicase-DNA-binding 1 gene (*CHD1*) on the Z and W sex chromosomes, using muscle tissue as a DNA source (see online supplementary material for detailed methods). The liver was weighed and divided for different types of analyses prior to freezing. To assess PFAS transfer to duckling tissues, concentrations were measured in liver subsamples. In brief, liver tissue was extracted with methanol containing 1% ammonium formate and internal standards, then analyzed using ultra-performance liquid chromatography tandem mass spectrometry. Online supplementary material Figure S1 illustrates the distribution of PFAS concentrations in liver samples from individuals in the present study ($n = 28$), representing a subset of ducklings from the larger study.

For RNA extraction, liver (~3 mm cube) was collected in a nuclease-free microcentrifuge tube prefilled with 700 µl QIAzol Lysis (Qiagen, Hilden, Germany) and a 5-mm stainless steel bead (Qiagen, Hilden, Germany) and immediately homogenized using a TissueLyser II (25 Hz, 3 min; Qiagen, Hilden, Germany). The homogenate was placed on dry ice and frozen at −80 °C. Heart and bursa of Fabricius samples were snap-frozen in liquid nitrogen. Immediately prior to RNA extraction, an approximate 3-mm cube subsample was taken from each tissue and homogenized using the TissueLyser II. Total RNA was isolated from a subset of liver, heart, and bursa tissues ($n = 4$ females per group, $n = 3$ males per group) using the miRNeasy Mini Kit (Qiagen, Hilden, Germany), according to the manufacturer's protocol.

RNA sequencing of liver

Sequencing of mRNA and small RNA was performed on liver samples from 28 mallard ducklings in the control group and the three exposure groups ($n = 4$ females per group, $n = 3$ males per group; online supplementary material Table S2). Library preparation and RNA sequencing of liver samples were performed by Novogene Europe (Cambridge, UK). The RNA quantity and quality were confirmed using NanoDrop spectrophotometry (NanoDrop Technologies, Wilmington, DE, USA), agarose gel electrophoresis, and the Agilent 5400 Fragment Analyzer system (Agilent

Technologies, Santa Clara, CA, USA). Messenger RNA was purified from total RNA using poly-T oligo-attached magnetic beads. After fragmentation, unstranded mRNA libraries were prepared using the Novogene PT042 NGS RNA Library Prep Set (Novogene Company, Cambridge, UK), followed by sequencing on NovaSeq X Plus 10B flow cells, generating approximately 20 million 150 bp paired-end reads per sample. Small RNA-stranded libraries were prepared using the NEBNext Multiplex Small RNA Library Prep Set for Illumina (New England Biolabs, Beverly, MA, USA) and sequenced on a NovaSeq 6000 SP flow cell, generating approximately 20 million 50 bp single-end reads per sample (online supplementary material Table S3).

mRNA bioinformatics pipeline

Raw data were quality-checked using FastQC v0.11.9 (Andrews, 2010), followed by adapter and quality trimming using fastp with default settings (Chen et al., 2018). Clean reads were mapped against the *A. platyrhynchos* genome assembly ZJU1.0 (GCA_015476345.1 GCF_015476345.1) using STAR (Dobin et al., 2013) with parameter outSAMtype BAM SortedByCoordinate (online supplementary material Table S3). Gene counts were obtained by applying featureCounts (v1.4.3; Liao et al., 2014) with default settings to the sorted BAM files.

microRNA bioinformatics pipeline

Libraries were pre-processed (3′ adapter-trimming, removing low-quality reads, low-complexity reads, and reads < 18 nt) and quality-checked using miRTrace (Ver. 1.0.1; Kang et al., 2018) in QC mode with default settings and with species set to chicken (*Gallus gallus*, gga). Of the 677,155,433 raw reads, 99% (669,564,360) passed miRTrace quality control, of which 447,747,604 were identified as miRNA reads. The miRTrace QC report file is available in the online supplementary material (pages 6–9, Figure S2). For de novo miRNA discovery, we used the genome-based discovery tool miRDeep2 (Friedländer et al., 2012). The mallard (*A. platyrhynchos*, assembly ZJU1.0, GenBank assembly GCA_015476345.1) was used as a reference genome for miRDeep2 and was indexed using the bowtie-build function (default settings; Langmead et al., 2009). The miRTrace quality control-passed reads were aligned against the indexed mallard genome using the miRDeep2 mapper module with parameters –d –c –i –j –l 18 –m. The mapper module output and known miRNA data from the four avian species in the miRBase repository (release 22.1; Ambros et al., 2003; Griffiths-Jones et al., 2006; Kozomara et al., 2019; Kozomara & Griffiths-Jones, 2014) were used to run the miRDeep2 module for de novo miRNA discovery with default parameters, followed by expression analysis using the miRDeep2 quantifier module (see online supplementary material page 1 for details).

Real-time quantitative polymerase chain reaction analysis

To investigate genes related to cellular stress response and inflammation in the heart (*AFT4*, *CAT*, *GPX1*, *HSPA2*, *HSP90AA1*, *NF-κB*, *NOX4*, *SOD1*, *SOD2*) and a subset of immune genes in bursa of Fabricius samples (*IL10RA*, *MDA5*, *NF-κB*, *RIG-I*, *TLR4*, *TLR7*, *TNF-α*, *TBK1*), we performed reverse transcription quantitative polymerase chain reaction (RT-qPCR). Gene expression changes identified in the liver by RNA sequencing were not validated by RT-qPCR in this study due to the comprehensive nature of sequencing, the broader focus of the investigation, and cost constraints.

Total RNA was reverse transcribed into complementary DNA (cDNA) using the QuantiTect Reverse Transcription Kit (Qiagen, Hilden, Germany). For some genes, we utilized published cDNA primer sequences (Chapman et al., 2016; Hua et al., 2018; Yang et al., 2021; Zhang et al., 2019). The remaining primers were designed in-house because they were either unavailable or did not show good efficiency or consistent melt curves in our experimental setup (online supplementary material Table S7). Primers were designed using Primer-BLAST (Ye et al., 2012).

Real-time quantitative polymerase chain reaction was conducted using LightCycler 480 SYBR Green I Master (Roche Molecular Systems, Switzerland) in a LightCycler 96 instrument (Roche Molecular Systems, Switzerland). For each primer pair, three cDNA technical replicates were used. The cycling protocol was as follows: preincubation at 95 °C for 10 min, followed by 40 amplification cycles consisting of denaturation at 95 °C for 15 s, annealing at 60 °C for 15 s, and extension at 72 °C for 15 s. After amplification, melting-curve analysis was performed, starting with a 60 s hold at 95 °C, followed by 30 s at 65 °C, and then continuous measurement from 65 °C to 97 °C at 1-s intervals. Finally, a cooling step was included at 37 °C for 30 s. Melting curves were inspected to confirm the presence of a single product, and negative controls and non-template controls were assessed for reagent purity. The qPCR products from primers designed in-house were run on a 3% agarose gel to confirm their length and specificity.

To quantify miRNAs in the heart (apl-miR-1-3p, apl-miR-133a-3p, apl-miR-21-5p, apl-miR-215-5p, and apl-miR-490-5p), first-strand cDNA was synthesized using the miRCURY LNA RT Kit (Qiagen, Hilden, Germany). The reaction was carried out at 42 °C for 60 min, followed by enzyme inactivation at 95 °C for 5 min using a T100 Gradient 96-well PCR Thermal Cycler (Bio-Rad, Hercules, CA, USA). Real-time quantitative polymerase chain reaction was performed with the miRCURY SYBR Green PCR Kit (Qiagen, Hilden, Germany) and miRCURY Locked Nucleic Acid (LNA)-enhanced qPCR assays (Qiagen, Hilden, Germany, online supplementary material Table S10). A U6 spliceosomal RNA was used for normalization. The following cycling protocol was used: an initial heat-activation step at 95 °C for 2 min, followed by 40 cycles of denaturation at 95 °C for 10 s, and combined annealing/extension at 56 °C for 60 s. A melting-curve analysis was conducted from 60 to 95 °C to verify product specificity.

Statistical and functional analysis of RNA sequencing data

Differential expression analysis for both mRNA and small RNA sequencing data was carried out using DESeq2 (Love et al., 2014) in R Ver. 4.3.0 (R Core Team, 2023). Genes were included in the analysis if they had more than 10 counts in at least three samples. To assess differences in gene expression between PFAS exposure groups, we used the "~Group" term (presented in the online supplementary material Figure S3 and Table S11). Sex-specific differences were extracted using the interaction term "~Sex*Group." Genes with multiple-testing adjusted (Benjamini & Hochberg, 1995) p-values < 0.05 and an absolute log2 fold change (log2FC) > 0.5 were defined as differentially expressed (DE). To visualize expression, counts were subjected to blind variance-stabilizing transformation. Figures were generated using the ggplot2 package (Wickham, 2011) in R.

Given the limited availability of functional annotations for duck genes, functional clustering and pathway enrichment analysis of differentially expressed genes (DEGs) were based on chicken orthologs. Gene Ontology (GO) enrichment analysis, including Kyoto Encyclopedia of Genes and Genomes (KEGG) pathway enrichment, was performed using the g:GOSt tool of g:Profiler (Kolberg et al., 2023), with *G. gallus* as the reference

organism. We set the false discovery rate threshold to < 0.05 to evaluate GO terms in the biological process, molecular function, and cellular component categories.

Targets of the DE miRNAs were predicted in silico using the sRNAtoolbox (Rueda et al., 2015) tool miRNAconsTarget that integrates miRanda (John et al., 2004), PITA (Kertesz et al., 2007), and TargetSpy (Sturm et al., 2010). MiRanda, PITA, and TargetSpy were run with default parameters against the 3′ UTR sequences of duck mRNAs.

Statistical analysis of RT-qPCR data

Raw quantification cycle values were obtained using the LightCycler 96 analysis software (Ver. 1.1; Roche Molecular Systems, Switzerland). The efficiency of each primer was calculated from the slopes of amplification curves and averaged for each gene using a window-of-linearity approach in the web-based tool LinRegPCR (Untergasser et al., 2021).

A stability analysis of six candidate reference genes (Chapman et al., 2016; *ACTB*, *GAPDH*, *NDUFA10*, *RPL4*, *RPS13*, *SDHA*) in heart and bursa of Fabricius samples was performed using BestKeeper (Pfaffl et al., 2004) and geNorm (Vandesompele et al., 2002) from the ctrlGene R package, along with NormFinder (Andersen et al., 2004). The results, presented in the online supplementary material Tables S8 and S9, indicate that *RPS13* is stably expressed in hearts, and *NDUFA10* and *RPS13* are stably expressed in the bursa in our experimental setup.

Relative quantification and statistical testing of RT-qPCR data were performed using the MCMC.qpcr package (Matz et al., 2013) in R Ver. 4.3.0 (R Core Team, 2023). Raw quantification cycle values were converted to molecular counts using the cq2counts function provided in the package. The molecular counts were modeled separately for each tissue type using the MCMC.qpcr function, which applies generalized linear mixed models under a Poisson-lognormal error distribution to assess the effects of PFAS exposure on the expression of each gene. The model fitting process involves a Bayesian Markov Chain Monte Carlo (MCMC) sampling scheme, which samples from the posterior distribution of model parameters to estimate gene expression levels. This approach accounts for both fixed effects (∼Group and ∼Sex:Group to investigate sex-specific effects) and random effects introduced by variation among the three technical replicates (used individually without averaging), effectively normalizing for differences in template input. Relative quantification was performed relative to the stably expressed reference genes specific to each organ for normalization (*RPS13* for heart mRNA, U6 spliceosomal RNA for heart miRNA, and *NDUFA10* and *RPS13* for Bursa mRNA) using the soft-normalization approach in MCMC.qpcr. Results are reported as posterior mean estimates of transcript levels, with gene expression changes presented as log2FC relative to the control group for consistency and comparison with RNA sequencing data. Each posterior mean is accompanied by a 95% credible interval, as calculated by the MCMC.qpcr package. Statistical significance was determined using *p*-values calculated from the posterior distribution, tested against a normal distribution using a z-score, and corrected for multiple testing (Benjamini & Hochberg, 1995). Gene expression changes with *p*-values < 0.05 were considered statistically significant. Diagnostic plots from MCMC.qpcr were used to assess model assumptions, including normality, homoscedasticity, and linearity. Figures were generated using the ggplot2 package (Wickham, 2011) in R.

Results

mRNA expression in liver

An overview of the sequencing quality and data processing metrics is available in the online supplementary material Table S3. After adapter-trimming, length-filtering, and quality-filtering, 604,785,915 clean reads remained. Of these clean reads, 79.4% uniquely mapped to the reference genome, with 14,841 genes successfully annotated against the reference genome out of a total of 25,165 genes in the *A. platyrhynchos* ZJU1.0 assembly. Comparisons between PFAS-exposed groups ($n = 7$ per group) and the control group ($n = 7$) revealed that five genes were upregulated (*CD36*, LOC113844342, *RPS21*, *SLCO1C1*, and *SPON1*), while five genes were downregulated (*BRICD5*, *HES4*, *IL10RA*, *PCSK1*, and *ITGA10*) in response to PFOS exposure (online supplementary material pages 1–4, Figures S3 and S4, Table S11). In the PFDoDS and PFECHS groups, no DEGs were found (online supplementary material Figure S3).

When accounting for sex ($n = 4$ females per group, $n = 3$ males per group) in the analysis, we observed sex-specific effects of PFAS exposure (Figure 1, see online supplementary material Tables S12–S15). Females exhibited distinct hepatic gene expression changes in response to PFDoDS and PFOS exposure (Figure 1A and C, see online supplementary material Tables S12 and S13), while hepatic gene expression differences were found in PFECHS- and PFOS-exposed males (Figure 1E and F, see online supplementary material Tables S14 and S15).

A downregulation of *PCSK1* was observed only in PFDoDS-exposed females (log2FC = −6.5, adj. *p*-value = 1.9e-08), but not in males. Additionally, in livers from PFDoDS-exposed females, *RPS21*, which encodes a component of the small 40S ribosomal subunit, was upregulated (log2FC = 5.5, adj. *p*-value = 2.1e-06). In PFOS-exposed females, *TEKT5* is strongly downregulated (log2FC = 6.53, adj. *p*-value = 0.048).

In PFECHS-exposed males, 16 genes were up-regulated, while 35 genes were down-regulated. Of the 51 DEGs, 37 genes could be mapped to GO terms and KEGG pathways in chicken, enabling further analysis. Among the downregulated genes, this analysis revealed significant enrichment of motifs from the transcription factors Nuclear Factor Erythroid 4 (NF-E4), Specificity protein 1 (Sp1), and Vitamin D Receptor (VDR; see online supplementary material Table S16), while no enrichment was observed among the upregulated genes.

In PFOS-exposed males, 10 genes were up-regulated, while 15 genes were down-regulated. Six genes (*MAP7D1*, *PARS2*, *SETX*, *TBC1D10A*, *TBK1*, and *TIGD5*) overlapped between the DEGs in PFECHS- and PFOS-exposed males.

microRNA expression in liver

The small RNA sequencing libraries generated from duck liver tissue ($n = 28$) were pooled to improve read depth for novel miRNA discovery. The miRDeep2 discovery module predicted 844 candidate miRNAs, with 474 passing a miRDeep2 score threshold of 4, corresponding to a signal-to-noise ratio of 9 (see online supplementary material Table S4). In total, we identified 183 conserved miRNAs belonging to 94 miRNA families and 6 novel miRNAs in the small RNA libraries (see online supplementary material Tables S5 and S6). Liver-specific miR-122-5p was the most highly expressed, representing 39% of the mapped reads, followed by miR-148-3p (18%) and let-7f-5p (4%) (see online supplementary material Figure S5).

No differences were found in hepatic miRNA expression between the control and PFAS-exposed groups (see online supplementary material Figures S6 and S7). However, we found a

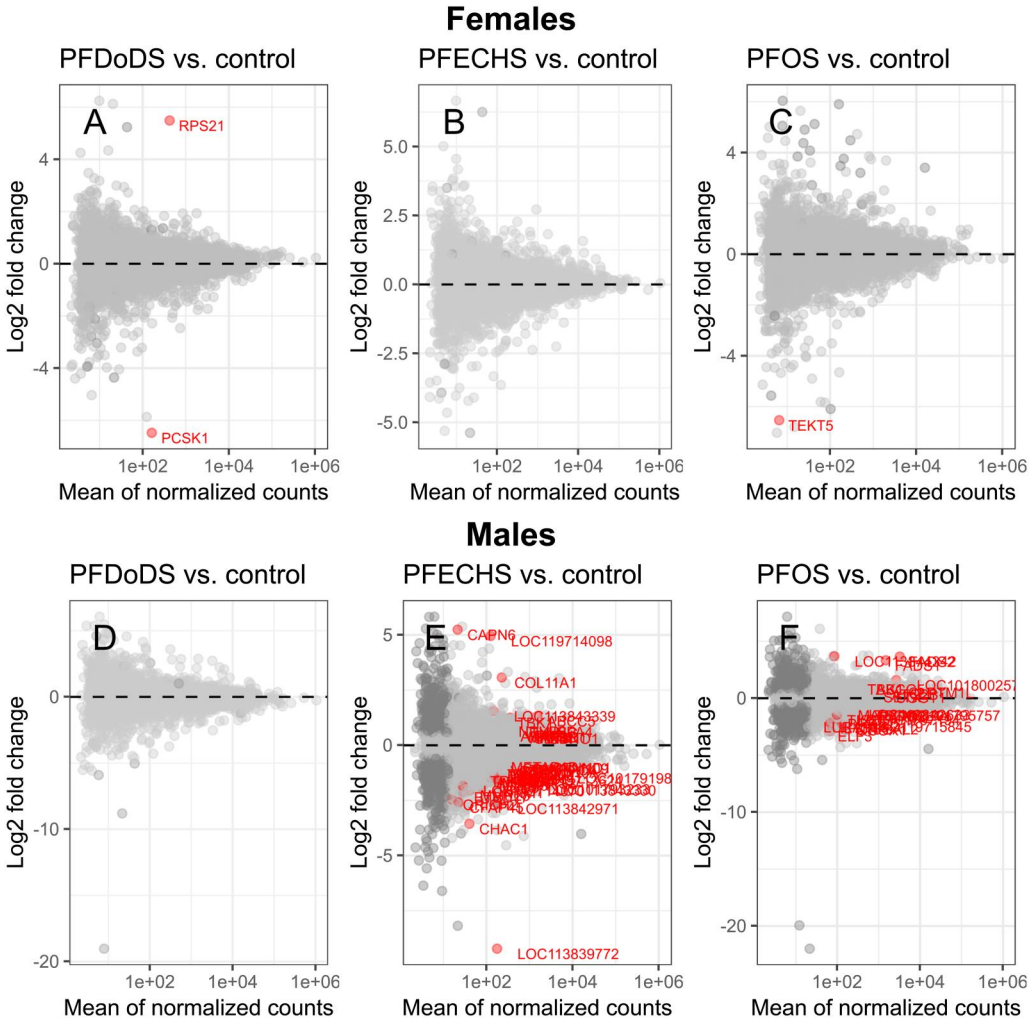

Figure 1. Log2 fold changes in mRNA expression versus the mean of normalized counts for mallard livers across different per- and polyfluoroalkyl substance exposure groups and sexes. Each panel represents a comparison between an exposure group and the control group. Exposure groups include perfluorododecane sulfonic acid (PFDoDS), perfluoro-4-ethylcyclohexane sulfonic acid (PFECHS), and perfluorooctanesulfonic acid (PFOS). Top panels (A–C): females ($n = 4$ per group). Bottom panels (D–F): males ($n = 3$ per group). Gray points represent genes that are not significantly differentially expressed (adjusted p-value ≥ 0.05 or absolute log2 fold change < 0.5), while red points indicate genes with significant differential expression (adjusted p-value < 0.05 and absolute log2 fold change ≥ 0.5).

sex-specific effect for miR-215-5p, which was upregulated in males exposed to PFDoDS compared with males in the control group (log2FC = 5.3, $p = 0.03$, Figure 2). Similar trends were found for males exposed to PFECHS (log2FC = 4.3, $p = 0.18$) and PFOS (log2FC = 2.6, $p = 0.51$), but these were not significant. Out of all the duck 3′ UTRs, 82 were consistently predicted to be targeted by apl-miR-215-5p by all three algorithms (miRanda, PITA, and TargetSpy). None of these correspond to genes that were DE in any of our comparisons. Four of the 82 genes (*ALCAM*, *ARHGEF39*, *TYMS*, and *ZBTB34*) are also listed as targets for human miR-215-5p in TargetScanHuman 8.0 (McGeary et al., 2019).

mRNA expression in heart

To assess potential cardiotoxicity of PFAS exposure, the expression of nine genes involved in the cellular stress response and inflammation were quantified in heart samples. No differences ($p > 0.05$) were found in any of the PFAS exposure groups (Figure 3, see online supplementary material Table S17). The expression of *CAT*, an enzyme involved in the neutralization of ROS, was lower in the PFOS group (log2FC = −0.83), with a marginal p-value ($p = 0.09$). For *HSPA2*, encoding a heat shock protein involved in cellular stress response and protein folding, showed small increases in expression across all exposure groups: PFDoDS (log2FC = 0.52, $p = 0.67$), PFECHS (log2FC = 0.63, $p = 0.58$), and PFOS (log2FC = 0.44, $p = 0.67$). For *SOD2*, an enzyme involved in mitigating oxidative stress, we observed small, marginally significant increases in expression in both PFDoDS (log2FC = 0.43, $p = 0.13$) and PFECHS (log2FC = 0.42, $p = 0.13$) groups. Stratifying by sex or examining sex-by-group interactions (see online supplementary material Figure S8 and Table S20), did not reveal any differences in gene expression ($p > 0.05$).

microRNA expression in heart

We measured the expression of four miRNAs (apl-miR-1-3p, apl-miR-21-5p, apl-miR-133a-3p, and apl-miR-490-5p) in heart tissue to assess their potential involvement in PFAS-induced cardiotoxicity. However, no differences ($p > 0.05$) in expression were observed across the PFAS exposure groups (see online supplementary material Figure S9 and Table S18). No differences in miRNA expression were found when stratifying by sex or examining sex-by-group interactions (see online supplementary material Figure S10 and Table S21).

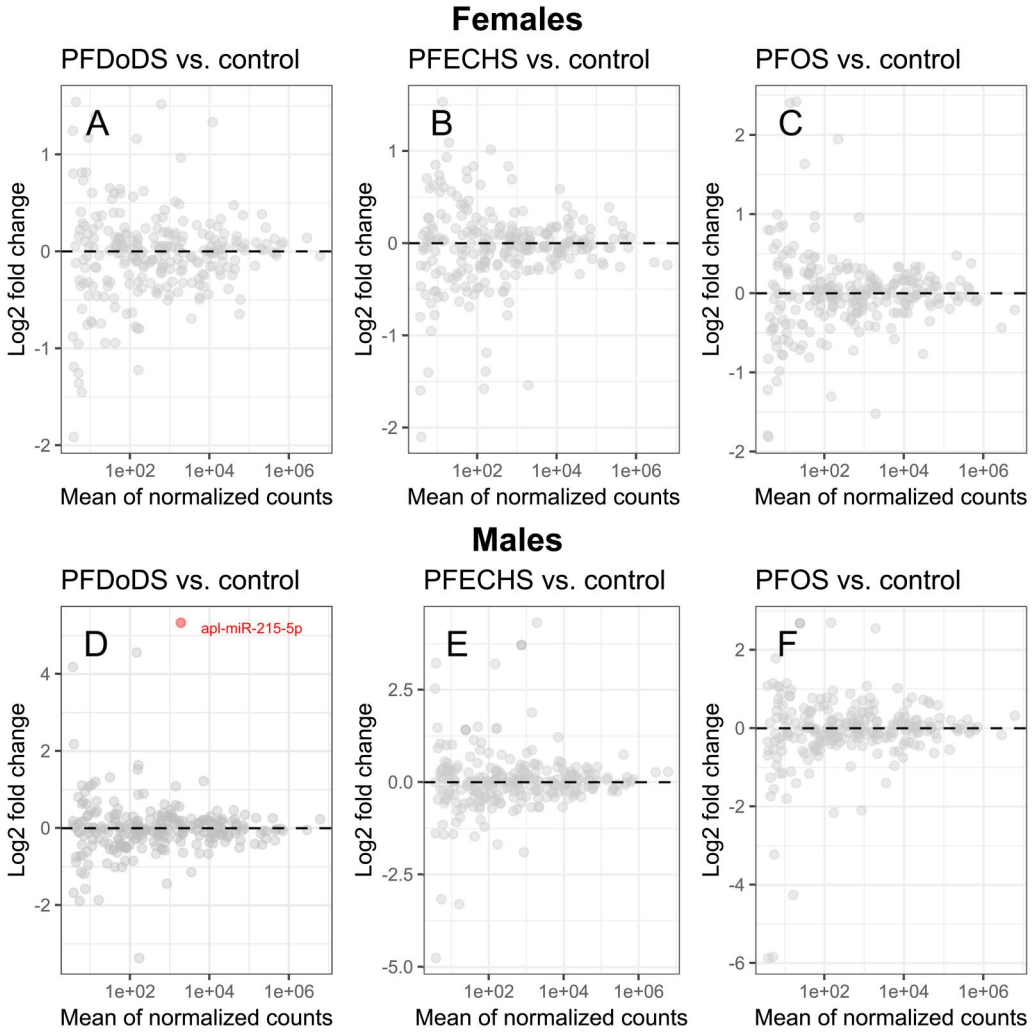

Figure 2. Log2 fold changes in microRNA expression versus the mean of normalized counts for mallard livers across different per- and polyfluoroalkyl substance exposure groups and sexes. Each panel represents a comparison between an exposure group and the control group. Exposure groups include perfluorododecane sulfonic acid (PFDoDS), perfluoro-4-ethylcyclohexane sulfonic acid (PFECHS), and perfluorooctanesulfonic acid (PFOS). Top panels (A–C): females ($n = 4$ per group). Bottom panels (D–F): males ($n = 3$ per group). Gray points represent genes that are not significantly differentially expressed (adjusted p-value ≥ 0.05 or absolute log2 fold change < 0.5), while red points indicate genes with significant differential expression (adjusted p-value < 0.05 and absolute log2 fold change ≥ 0.5).

mRNA expression in the bursa of Fabricius

To assess potential immunomodulation of PFAS exposure, the expression of eight immune response genes was quantified in bursa samples (Figure 4, see online supplementary material Table S19). Small changes were observed for several genes across the PFAS exposure groups. The *IL10RA*, a receptor subunit that forms the interleukin 10 receptor complex (involved in anti-inflammatory signaling), exhibited reduced expression in the PFOS group (log2FC = −0.79), though this change was not significant ($p = 0.24$). The *RIG-I* (a pattern recognition receptor involved in the detection of viral RNA) expression was upregulated in the PFDoDS (log2FC = 0.42, $p = 0.03$), PFECHS (log2FC = 0.45, $p = 0.03$), and PFOS (log2FC = 0.49, $p = 0.03$) groups. When stratified by sex, this increase appeared to be driven by males, though no significant difference was detected ($p = 0.09$ for PFDoDS; see online supplementary material Figure S11 and Table S22). The *MDA5* (a *RIG-I*-like receptor [RLR]) was also increased in the PFECHS (log2FC = 0.36, $p = 0.07$) and PFOS (log2FC = 0.37, $p = 0.07$) exposure groups, though these changes were only marginally significant. Although *TBK1* expression did not differ across exposure groups overall, sex-stratified analysis revealed a marginally significant difference between males and females (log2FC = −1.66, $p = 0.10$), with higher expression observed in females (see online supplementary material Figure S11 and Table S22).

Discussion

In this study, we investigated the transcriptomic responses in ducklings exposed in ovo to the emerging PFAS compounds PFDoDS and PFECHS, alongside the legacy PFOS. By examining tissues immediately after hatching, we focus on molecular changes during a critical developmental stage, providing insights into the early-life effects of PFAS exposure. Despite growing concern, there is limited research on the impacts of PFAS exposure during early-life stages, particularly regarding the sublethal effects on birds. The findings discussed here reveal the first detailed information regarding gene expression changes in mallard liver, heart, and bursa of Fabricius in response to PFDoDS and PFECHS exposure.

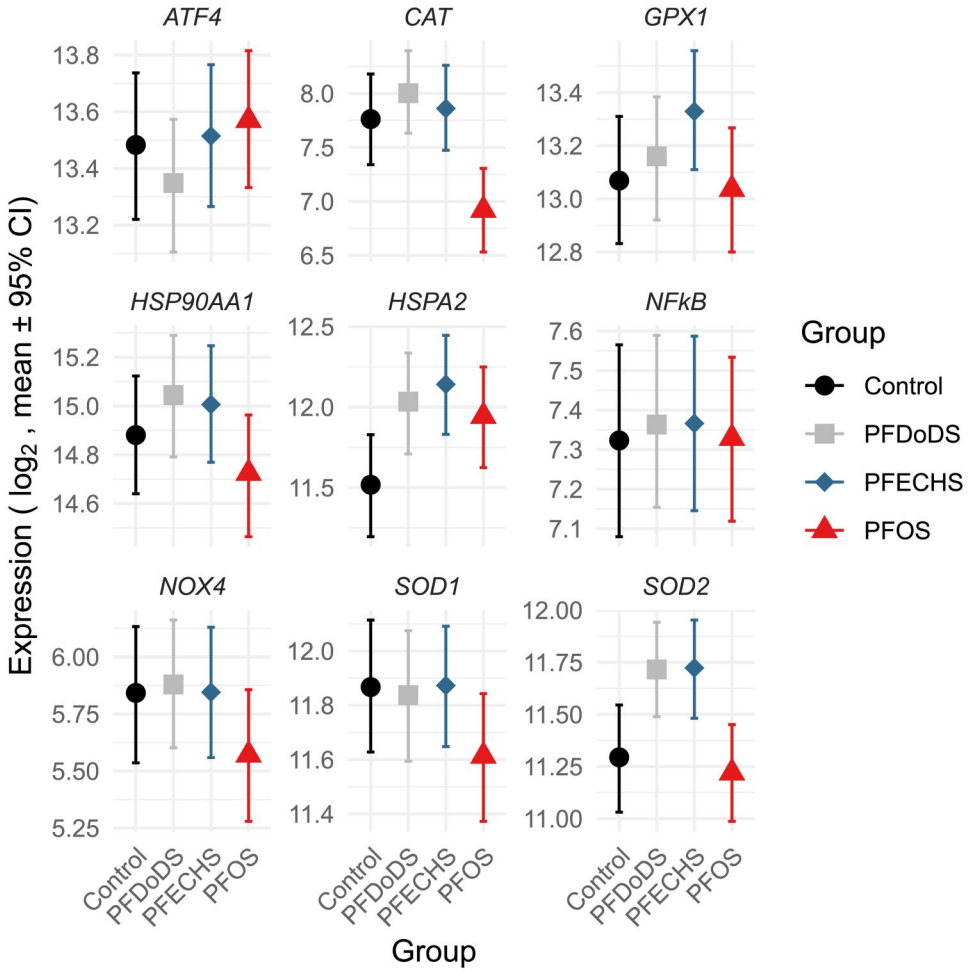

Figure 3. mRNA expression in heart across per- and polyfluoroalkyl substance-exposed groups ($n = 7$ per group). Exposure groups include perfluorododecane sulfonic acid (PFDoDS), perfluoro-4-ethylcyclohexane sulfonic acid (PFECHS), and perfluorooctanesulfonic acid (PFOS). Points represent the group means of normalized gene expression (log_2 scale), and whiskers indicate the 95% credible intervals (CI) of the means, derived from Markov Chain Monte Carlo sampling. No significant differences were observed.

mRNA expression in liver

The liver, due to its central role in detoxification and metabolic processes, is likely to respond to chemical exposure relatively early in development, as it is already active in ovo and continues functioning post-hatching (Noble & Cocchi, 1990). No gene expression changes were detected for PFDoDS and PFECHS in the liver when sex was not considered; only PFOS exposure led to differential gene expression (see online supplementary Figure S3, Table S11). As PFOS was included primarily as a comparison for the two emerging PFAS, the PFOS results are discussed in detail in the online supplementary material. Liver concentrations of PFECHS and PFOS were nearly twice as high as those of PFDoDS (see online supplemental material Figure S1), which may partly explain the absence of DEGs for PFDoDS. While the lack of gene expression changes for PFECHS is consistent with previous studies showing fewer transcriptional effects compared to PFOS (Houde et al., 2016; Mahoney et al., 2024), it is possible that subtle or sex-specific responses were masked in the combined analysis. These findings highlight the importance of considering both internal dose and biological variables such as sex in toxicogenomic assessments.

Even for PFOS, only 10 DEGs were identified, which is a relatively low number. After sex-stratified analysis, additional DEGs were observed, but the numbers remained modest across all exposure groups. The overlapping DEGs between PFOS- and PFECHS-exposed males suggest shared transcriptional effects among these sulfonated PFAS, with consistent directions of expression change indicating potentially common modes of action. While 80 ng/g egg is at the upper end (for PFDoDS) or slightly above (for PFECHS) concentrations measured in wild bird eggs (see online supplementary material Table S1), it remains lower than the concentrations typically used in experimental toxicology studies. For example, others have used PFOS concentrations ranging from 150 to 1500 ng/g egg (Briels et al., 2018), 0.1 to 1 μg/g egg (Geng et al., 2019), or 0.5 to 3 μg/g egg (Mattsson et al., 2019). These higher concentrations are more likely to induce widespread changes in gene expression (Liu et al., 2022). Dose–response analysis of high-throughput biochemical data indicates genes induced at low doses typically correspond to the disruption of specific biomolecular pathways, while higher-dose effects typically involve a broader range of affected pathways, likely reflecting cytotoxicity, cell stress, or general disruption of molecular machinery (Judson et al., 2016). Hence, the genes identified here may provide a better insight into the initial molecular processes affected by PFAS exposure.

Most sex-specific effects in gene expression are typically driven by hormones and are more likely to become evident after the maturation and development of the reproductive system (Blencowe et al., 2022). However, sex differences in gene expression can also arise from other mechanisms, such as sex chromosome-linked

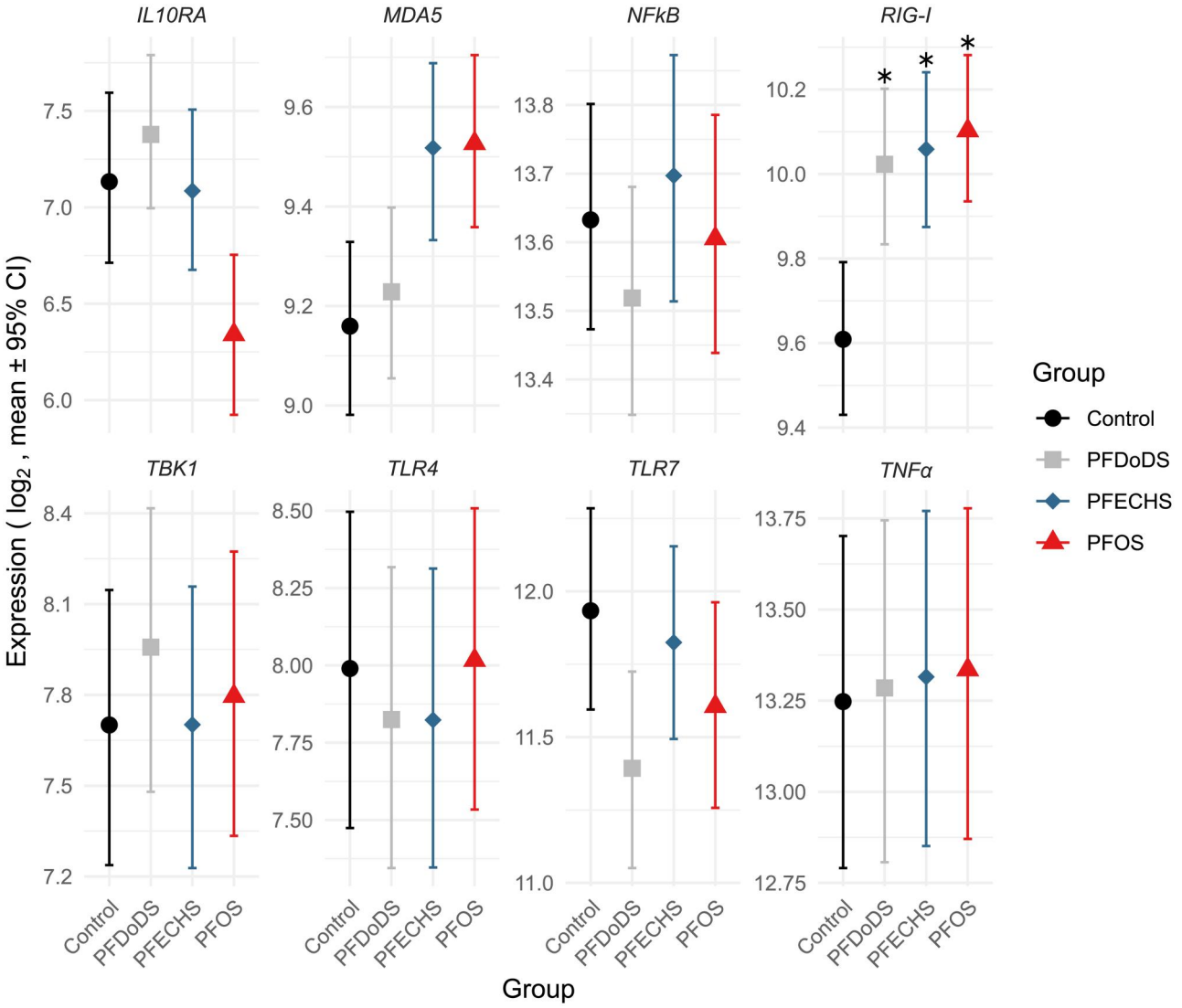

Figure 4. mRNA expression in bursa of Fabricius across per- and polyfluoroalkyl substance-exposed groups ($n = 7$ per group). Exposure groups include perfluorododecane sulfonic acid (PFDoDS), perfluoro-4-ethylcyclohexane sulfonic acid (PFECHS), and perfluorooctanesulfonic acid (PFOS). Points represent the group means of normalized gene expression (log_2 scale), and whiskers indicate the 95% credible intervals (CI) of the means, derived from Markov Chain Monte Carlo sampling. *Indicates statistical significance.

genes or epigenetic regulation (Shepherd et al., 2020). Of all the DEGs identified in this study, only *PCSK1* is located on a sex chromosome, and it was significantly higher in livers from males than females, regardless of their exposure status (log2FC = 2.99, adj. *p*-value = 3.58e-04). The *PCSK1* DEG encodes an enzyme that processes a range of prohormones involved in metabolic regulation (Stijnen et al., 2016). In PFDoDS-exposed females, downregulation of *PCSK1* was observed, but no such effect was seen in males. A similar trend was found in PFOS-exposed ducklings when sex was not considered. As *PCSK1* is located on the Z chromosome, the observed sex-specific downregulation in females may reflect genetic differences between males (ZZ) and females (ZW), suggesting a role for sex-chromosome-linked genes in mediating these effects. In humans, *PCSK1* deficiency or mutation leads to maladaptive diarrhea in newborns and obesity, typically accompanied by hyperphagia in later life (Stijnen et al., 2016). In domestic birds, including ducks, PCSK1 has gained attention for its role in abdominal fat deposition and muscle growth (Wang et al., 2017). The PCSK1 substrates, including proinsulin, proglucagon, and proopiomelanocortin, play key roles in nutrient absorption, metabolism, and appetite regulation. Obesity has been attributed to defective proopiomelanocortin processing and disruption of the melanocortin system (Lloyd et al., 2006). The potential interference of PFAS with hepatic lipid metabolism is particularly relevant for wild birds, in which adequate fat storage is crucial for migration and reproductive cycles. The effects of PFDoDS on *PCSK1* expression in duck liver could be particularly relevant for wild birds, especially females, that may undertake longer migrations than males (Carbone & Owen, 1995). Disruptions in metabolic pathways, such as those involving *PCSK1*, could alter their ability to store fat efficiently, potentially affecting their seasonal behaviors, reproductive success, overall fitness, and survival.

With only a small number of DEGs identified, performing GO/KEGG pathway analysis is suboptimal, as the risk of false-positive terms increases. Therefore, these results should be interpreted with caution. Nevertheless, the enrichment of transcription factor binding motifs for NF-E4, Sp1, and VDR among downregulated genes in PFECHS-exposed males are biologically relevant and aligns with known disruptions caused by PFAS exposure. Notably, Sp1 has previously been implicated with PFAS

toxicity in human liver cells, in which perfluorooctanoic acid (PFOA) exposure induced hypermethylation of the glutathione-S-transferase Pi promoter specifically at the Sp1-binding site, highlighting a possible mechanism of epigenetically mediated transcriptional repression (Tian et al., 2012). An in silico analysis predicted that several PFAS compounds could interact strongly with VDR, with PFECHS showing a moderate docking score of −7.186 kcal/mol compared to −11.81 kcal/mol for the natural ligand, suggesting potential for partial VDR interference (Singam et al., 2023). Supporting this, in vitro studies show PFOA can disrupt vitamin D signaling by competitively binding VDR and inhibiting downstream gene expression (Di Nisio et al., 2020). In light of the observed *RIG-I* upregulation in the bursa, it is notable that VDR typically suppresses pro-inflammatory cytokines, including IFN-γ (Staeva-Vieira & Freedman, 2002), a known inducer of *RIG-I* (Spalluto et al., 2017). These findings support a mechanism in which PFAS binding to VDR impairs its immunoregulatory role, increasing IFN-γ, and thereby promoting *RIG-I* expression in immune tissues. Although NF-E4 has not previously been associated with PFAS, it has been identified in the MDA5 promoter region in chickens (Zhang et al., 2016), suggesting a potential regulatory role in antiviral gene expression that warrants further investigation in the context of PFAS-induced immunomodulation.

microRNA expression in liver

Hepatic miRNA expression was largely unaffected by any of the PFAS in our study, except in males exposed to PFDoDS, in which miR-215-5p was upregulated. Because the PFDoDS-exposed males showed no changes in their hepatic mRNA expression, the usual approach of comparing DE miRNAs with DE mRNAs to investigate potential miRNA–mRNA interactions is not applicable in this context. The difference in mRNA expression between PFDoDS-exposed males and females, in which *RPS21* and *PCKS1* are dysregulated, is unlikely to be related to miR-215-5p, as these genes are neither known nor computationally predicted targets of this miRNA.

Mir-215 is a well-studied miRNA, notably linked to various cancers and human diseases, influencing tumor initiation and progression (reviewed by Vychytilova-Faltejskova and Slaby [2019]). In the context of PFAS, miR-215-5p has been identified through in silico data mining as potentially involved in polycystic ovary syndrome progression, particularly through cell cycle regulation (Xu et al., 2024). Additionally, miR-215 has been shown to induce autophagy in chicken cardiomyocytes, leading to myocardial injury through PI3K/AKT/TOR and ROS-MAPK pathways (Cai et al., 2019). In our study, the upregulation of miR-215-5p in PFDoDS-exposed male ducklings suggests potential implications for cellular stress response mechanisms, warranting further investigation.

mRNA expression in heart

In the heart, we observed marginally significant, small changes in the expression of oxidative stress-related genes *CAT* and *SOD2*. Increased ROS production is a well-established effect of PFAS exposure, and while many studies report this, the trends in gene expression of antioxidant enzymes across the literature vary (Bonato et al., 2020). The decrease in *CAT* expression in PFOS-exposed ducklings is consistent with previous research in adult male rats, where PFOS oral gavage (20 mg/kg/day for 4 weeks) resulted in a significant decrease in both catalase (CAT) activity and superoxide dismutase in the heart (Mandour et al., 2023). Our findings suggest that the previously reported decrease in antioxidant activity in the heart following PFOS exposure may occur at the level of mRNA expression. However, a recent study using a ligand-docking approach predicted that PFOS can potentially bind with antioxidant enzymes, including CAT (Rajak & Ganguly, 2023), suggesting that multiple mechanisms are likely at play.

The modest increase in *HSPA2* across all three exposure groups suggests a shared mechanism related to the cellular stress response. These increases may indicate an adaptive stress response, as the aforementioned study in rats reported an increase in the area percent of *HSPA2* immunoexpression in the PFOS-exposed hearts (Mandour et al., 2023), supporting HSPA2's role in the PFAS response. These findings should also be considered in the context of the pronounced upregulation of heat shock protein 30C-like (LOC119714098), alongside *HSPA4*, observed in the livers of PFECHS-exposed males, further supporting the presence of a cellular stress response induced by chemical exposure (Heikkila, 2017).

microRNA expression in heart

The investigated miRNAs miR-1-3p and miR-133a-3p are heart-specific miRNAs involved in cardiac development and function (Gu et al., 2014), while miR-21-5p plays a role in regulating inflammation and fibrosis (Surina et al., 2021). Levels of apl-miR-215-5p, which was upregulated in livers from PFDoDS-exposed males, were below the detection limits of our assay, precluding further analysis. MiR-490-5p has been implicated in PFAS-induced effects in chicken hearts (Guo et al., 2022). The lack of observable effects may be due to low exposure concentrations or the possibility that miR-1 and miR-133 are more sensitive to PFAS earlier in development, when they play critical roles in cardiomyocyte differentiation (Wystub et al., 2013).

mRNA expression in the bursa of Fabricius

We evaluated the potential immunotoxicity of PFDoDS and PFECHS exposure by quantifying the expression of eight immune response genes in the bursa of Fabricius. At the early post-hatching stage, the bursa is still developing, and the ducklings retain maternal antibodies from the yolk sac (Schat et al., 2014). As a result, the immune system may not yet be sufficiently mature to exhibit measurable transcriptomic changes during this period. Nevertheless, our results indicate that exposure to PFDoDS, PFECHS, and PFOS leads to small but significant increases in the expression of *RIG-I*, a key component of the innate immune system involved in pathogen recognition and antiviral responses. Notably, chickens lack a functional *RIG-I* gene (Magor et al., 2013), highlighting the value of ducks as a model organism for studying immunotoxic effects on antiviral immune pathways. Another member of the RLR family, *MDA5*, showed similar but non-significant increases in the PFECHS and PFOS groups.

The RIG-I-like receptors detect pathogen-associated molecular patterns, particularly viral double-stranded RNA, triggering the expression of type I interferons (IFNα and IFNβ) and other pro-inflammatory cytokines during early stages of viral infection (Brisse & Ly, 2019). In zebrafish larvae, exposure to PFOA, PFOS, hexafluoropropylene oxide dimer acid, and PFECHS activated RLRs and downstream immune genes (Yao et al., 2024). Molecular docking revealed strong interactions between these PFAS and RIG-I, with PFECHS showing stronger binding to RIG-I than PFOS. Similarly, a study on the emerging polyfluorinated compound Nafion by-product 2 demonstrated that exposure in zebrafish disrupts intestinal homeostasis and is associated with activation of the RLR signaling pathway (Gui et al., 2023). These findings suggest that novel PFAS, like PFDoDS and PFECHS, may interfere with the immune system by activating the RLR signaling pathway, possibly through binding to pattern recognition receptors such as RIG-I.

The seemingly more pronounced *RIG-I* upregulation in males than in females suggests potential sex-specific sensitivity to PFAS-induced immune modulation, with males potentially more susceptible to PFAS-mediated activation of antiviral pathways in lymphoid tissues. However, the observation that *TBK1* expression appears higher in PFOS-exposed females than in males contradicts this notion. TBK1 is a key regulator in antiviral responses and has been observed to be downregulated in livers from PFOS-exposed mice, supporting its potential involvement in PFAS-induced inflammatory pathways (Beggs et al., 2016). Recently, TBK1's role in a PFDA-induced inflammatory response pathway was confirmed (Cui et al., 2024). Importantly, TBK1 is recruited downstream of RIG-I following mitochondrial antiviral signaling activation, where it phosphorylates IRF3 and IRF7, leading to the production of type I IFNs (Seth et al., 2005), underscoring its role in propagating RIG-I-mediated antiviral signaling. To complicate matters, we observed tissue-specific differences in the effects of PFAS on *TBK1* expression. Specifically, in livers from PFOS- and PFECHS-exposed males (but not females), *TBK1* expression was significantly upregulated (see online supplementary material Figure S3 and Tables S12–S15). This suggests that the response to PFAS exposure may differ not only by sex but also by tissue type, highlighting the complexity of PFAS-induced immunomodulation. Further investigation is needed to determine whether these transcriptional changes translate into functional alterations in immune competence and whether they persist across developmental stages.

Although the hatchlings in our study were likely protected by maternal antibodies, the upregulation of these genes may reflect an early disruption in immune system development, potentially influencing the immune system's ability to respond to future pathogens. The lack of significant changes in other immune-related genes, such as *NF-κB*, *TLR4*, *TLR7*, and *TNF-α*, suggests that PFAS exposure may specifically impact antiviral pathways in newly hatched ducklings rather than broader immune activation.

Limitations and future perspectives

Our data support the hypothesis that in ovo exposure to PFDoDS and PFECHS can affect gene expression at concentrations approaching or slightly exceeding those currently reported in wild bird eggs. While PFDoDS concentrations align with the upper end of environmental measurements, the dose used for PFECHS exceeds currently known environmental concentrations, though continued use and environmental persistence could make such concentrations increasingly relevant over time. In particular, the effects on genes related to metabolism and immune function are concerning, as dysregulation of these pathways could impair critical physiological processes. Disruptions in metabolic and immune functions could compromise the development and overall health of the ducklings, highlighting the potential risks of maternal transfer of these substances into eggs.

It is important to note that in natural environments, wild birds are exposed to complex mixtures of PFAS and other chemicals, which may lead to additive or synergistic interactions that increase the overall risk. Although the fold changes in gene expression observed in the heart and bursa of the ducklings were relatively small, their relevance must be considered in the context of these complex mixtures (Ojo et al., 2021). The emerging PFAS compounds investigated in this study could be contributing to mixture effects, potentially exacerbating the biological impacts observed, even if individual compounds show modest effects in isolation. Future studies should aim to include environmentally relevant PFAS mixtures and dose–response designs to better reflect real-world exposure scenarios.

Furthermore, we only selected ducklings that successfully pipped and hatched from their eggs for transcriptomic analysis. This selection process may have inadvertently favored individuals that were less affected by PFAS exposure, as it is possible that those most severely impacted by the compounds died in the egg or failed to hatch. This potential selection bias should be considered when interpreting the results, as it is possible that the full extent of PFAS-induced developmental effects could be more pronounced in individuals that did not hatch.

The relatively small sample size ($n = 7$ per group) in the present study may have reduced the statistical power of the findings. However, both the costs associated with larger sample sizes and the ethical considerations regarding the number of animals used played a role in the study's design. While the primary aim was to explore PFDoDS- and PFECHS-induced transcriptomic changes, the most pronounced effects were observed in PFOS-exposed animals. As such, we did not perform RT-qPCR validation of hepatic gene expression. However, future research could validate specific genes to further support the transcriptomic findings while also examining the effects of PFAS exposure at different developmental stages and investigating sex-specific differences in response.

While the transcriptomic responses to these two emerging PFAS compounds showed some similarities to PFOS, particularly in immune-related genes such as *RIG-I* and *MDA5*, these similarities were not observed across all genes. These results suggest that legacy and replacement PFAS may affect similar biological pathways, although the full range of mechanisms of action for the emerging compounds remains to be further elucidated.

In addition to gene expression studies, it is important to explore downstream effects to confirm an adverse outcome pathway, as DEGs may not always reflect a specific toxic response but can indicate broader biological reactions to stressors (Snell et al., 2003). Future studies should employ multi-omics approaches to gain a more comprehensive understanding of emerging PFAS exposure. However, numerous studies, including our own and those summarized in the European Chemicals Agency's proposal for a PFAS restriction (European Chemicals Agency, 2023), have already identified similar effects between emerging and legacy PFAS for some endpoints, suggesting that replacement PFAS may not be suitable alternatives to legacy compounds. This further supports the case for a class-wide PFAS ban. Given the uncertainties surrounding their long-term impact, the precautionary principle should guide future management and regulation of these compounds.

Supplementary material

Supplementary material is available online at *Environmental Toxicology and Chemistry*.

Data availability

Raw reads have been deposited in the European Nucleotide Archive under accession number PRJEB70938 (ERP155840; sample accession numbers in online supplementary material Table S1). Bioinformatics scripts, raw qPCR data, and data processing scripts (R code) are available on DataverseNO (https://doi.org/10.18710/CZLZ0O).

Author contributions

Anne-Fleur Brand (Conceptualization, Data curation, Formal analysis, Investigation, Methodology, Validation, Visualization, Writing—original draft), Silje S. Peterson (Conceptualization,

Investigation, Writing—review & editing), Louisa M.S. Günzel (Data curation, Formal analysis, Investigation, Validation, Writing—review & editing), Kang Nian Yap (Investigation, Writing—review & editing), Tomasz Maciej Ciesielski (Investigation, Methodology, Writing—review & editing), Céline Arzel (Conceptualization, Funding acquisition, Investigation, Methodology, Project administration, Writing—review & editing), and Veerle L.B. Jaspers (Conceptualization, Funding acquisition, Investigation, Methodology, Project administration, Resources, Supervision, Writing—review & editing)

Funding

Funding was obtained through the COAST IMPACT project (Norwegian Research Council grant number 302205, attributed to V.L.B.J.) and the DISRUPT project (Research Council of Finland, grant numbers 333400 and 336261, attributed to C.A.). The authors would also like to thank the MatKat Foundation for awarding funding to L.M.S.G., which supported her research.

Conflicts of interest

The authors have no relevant financial or non-financial interests to disclose.

Ethical statement

All experimental procedures involving animals were approved by the Norwegian Food Safety Authority (Mattilsynet; FOTS ID 30237) and carried out at the animal laboratory facilities of the Department of Biology at NTNU in Norway.

Disclaimer

During the preparation of this work, the author used ChatGPT to assist in refining specific sections of the manuscript, including sentence structure and enhancing clarity. After using this tool, the author reviewed and edited the content as needed and takes full responsibility for the content of the publication.

Acknowledgments

The authors thank R. Røsbak and G. Stavik Eggen for their assistance with various aspects of the in ovo experiment.

References

Ambros, V., Bartel, B., Bartel, D. P., Burge, C. B., Carrington, J. C., Chen, X., Dreyfuss, G., Eddy, S. R., Griffiths-Jones, S., Marshall, M., Matzke, M., Ruvkun, G., & Tuschl, T. (2003). A uniform system for microRNA annotation. *RNA*, *9*, 277–279. https://doi.org/10.1261/rna.2183803

Andersen, C. L., Jensen, J. L., & Ørntoft, T. F. (2004). Normalization of real-time quantitative reverse transcription-PCR data: A model-based variance estimation approach to identify genes suited for normalization, applied to bladder and colon cancer data sets. *Cancer Research*, *64*, 5245–5250. https://doi.org/10.1158/0008-5472.CAN-04-0496

Andrews, S. (2010). FastQC: A quality control tool for high throughput sequence data. In *Babraham bioinformatics*. Babraham Institute. http://www.bioinformatics.babraham.ac.uk/projects/fastqc/

Antonopoulou, M., Spyrou, A., Tzamaria, A., Efthimiou, I., & Triantafyllidis, V. (2024). Current state of knowledge of environmental occurrence, toxic effects, and advanced treatment of PFOS and PFOA. *The Science of the Total Environment*, *913*, 169332. https://doi.org/10.1016/j.scitotenv.2023.169332

Bartel, D. P. (2004). MicroRNAs: Genomics, biogenesis, mechanism, and function. *Cell*, *116*, 281–297. https://doi.org/10.1016/s0092-8674(04)00045-5

Beggs, K. M., McGreal, S. R., McCarthy, A., Gunewardena, S., Lampe, J. N., Lau, C., & Apte, U. (2016). The role of hepatocyte nuclear factor 4-alpha in perfluorooctanoic acid-and perfluorooctanesulfonic acid-induced hepatocellular dysfunction. *Toxicology and Applied Pharmacology*, *304*, 18–29. https://doi.org/10.1016/j.taap.2016.05.001

Benjamini, Y., & Hochberg, Y. (1995). Controlling the false discovery rate: A practical and powerful approach to multiple testing. *Journal of the Royal Statistical Society: Series B (Methodological)*, *57*, 289–300. https://doi.org/10.1111/j.2517-6161.1995.tb02031.x

Blencowe, M., Chen, X., Zhao, Y., Itoh, Y., McQuillen, C. N., Han, Y., Shou, B. L., McClusky, R., Reue, K., Arnold, A. P., & Yang, X. (2022). Relative contributions of sex hormones, sex chromosomes, and gonads to sex differences in tissue gene regulation. *Genome Research*, *32*, 807–824. https://doi.org/10.1101/gr.275965.121

Bonato, M., Corrà, F., Bellio, M., Guidolin, L., Tallandini, L., Irato, P., & Santovito, G. (2020). PFAS environmental pollution and antioxidant responses: An overview of the impact on human field. *International Journal of Environmental Research and Public Health*, *17*, 8020. https://doi.org/10.3390/ijerph17218020

Briels, N., Ciesielski, T. M., Herzke, D., & Jaspers, V. L. (2018). Developmental toxicity of perfluorooctanesulfonate (PFOS) and its chlorinated polyfluoroalkyl ether sulfonate alternative F-53B in the domestic chicken. *Environmental Science & Technology*, *52*, 12859–12867. https://doi.org/10.1021/acs.est.8b04749

Brisse, M., & Ly, H. (2019). Comparative structure and function analysis of the RIG-I-like receptors: RIG-I and MDA5. *Frontiers in Immunology*, *10*, 1586. https://doi.org/10.3389/fimmu.2019.01586

Brunström, B., & Örberg, J. (1982). A method for studying embryotoxicity of lipophilic substances experimentally introduced into hens' eggs. *Ambio*, *11*, 209–211. https://www.jstor.org/stable/4312798

Cai, J., Yang, J., Liu, Q., Gong, Y., Zhang, Y., Zheng, Y., Yu, D., & Zhang, Z. (2019). Mir-215-5p induces autophagy by targeting PI3K and activating ROS-mediated MAPK pathways in cardiomyocytes of chicken. *Journal of Inorganic Biochemistry*, *193*, 60–69. https://doi.org/10.1016/j.jinorgbio.2019.01.010

Carbone, C., & Owen, M. (1995). Differential migration of the sexes of Pochard *Aythya ferina*: Results from a European survey. *Wildfowl*, *46*, 99–108. https://wildfowl.wwt.org.uk/index.php/wildfowl/article/view/973

Chapman, J. R., Helin, A. S., Wille, M., Atterby, C., Järhult, J. D., Fridlund, J. S., & Waldenström, J. (2016). A panel of stably expressed reference genes for real-time qPCR gene expression studies of mallards (*Anas platyrhynchos*). *PloS One*, *11*, e0149454. https://doi.org/10.1371/journal.pone.0149454

Chen, S., Zhou, Y., Chen, Y., & Gu, J. (2018). fastp: An ultra-fast all-in-one FASTQ preprocessor. *Bioinformatics*, *34*, i884–i890. https://doi.org/10.1093/bioinformatics/bty560

Cui, Z., Yuan, X., Wang, Y., Liu, Z., Fei, X., Chen, K., Shen, H.-M., Wu, Y., & Xia, D. (2024). Environmentally relevant level of PFDA exacerbates intestinal inflammation by activating the cGAS/STING/NF-κB signaling pathway. *The Science of the Total Environment*, *954*, 176786. https://doi.org/10.1016/j.scitotenv.2024.176786

De Silva, A. O., Spencer, C., Scott, B. F., Backus, S., & Muir, D. C. (2011). Detection of a cyclic perfluorinated acid, perfluoroethylcyclohexane sulfonate, in the Great Lakes of North America. *Environmental Science & Technology*, *45*, 8060–8066. https://doi.org/10.1021/es200135c

Di Nisio, A., Rocca, M. S., De Toni, L., Sabovic, I., Guidolin, D., Dall'Acqua, S., Acquasaliente, L., De Filippis, V., Plebani, M., & Foresta, C. (2020). Endocrine disruption of vitamin D activity by perfluoro-octanoic acid (PFOA). *Scientific Reports*, *10*, 16789. https://doi.org/10.1038/s41598-020-74026-8

Dobin, A., Davis, C. A., Schlesinger, F., Drenkow, J., Zaleski, C., Jha, S., Batut, P., Chaisson, M., & Gingeras, T. R. (2013). STAR: Ultrafast universal RNA-seq aligner. *Bioinformatics*, *29*, 15–21. https://doi.org/10.1093/bioinformatics/bts635

Dong, H., Curran, I., Williams, A., Bondy, G., Yauk, C. L., & Wade, M. G. (2016). Hepatic miRNA profiles and thyroid hormone homeostasis in rats exposed to dietary potassium perfluorooctanesulfonate (PFOS). *Environmental Toxicology and Pharmacology*, *41*, 201–210. https://doi.org/10.1016/j.etap.2015.12.009

European Chemicals Agency (2023). *Annex to the ANNEX XV restriction report: Proposal for a restriction—Per- and polyfluoroalkyl substances (PFASs)*. https://echa.europa.eu/documents/10162/bc038c71-da3e-91a8-68c1-f52f8f0974dd

Friedländer, M. R., Mackowiak, S. D., Li, N., Chen, W., & Rajewsky, N. (2012). miRDeep2 accurately identifies known and hundreds of novel microRNA genes in seven animal clades. *Nucleic Acids Research*, *40*, 37–52. https://doi.org/10.1093/nar/gkr688

Frøyland, S. H. (2022). *Per-and polyfluoroalkyl substances (PFASs) concentrations over the laying sequence in eggs of the common eider (Somateria mollissima) from the Baltic Sea in relation to sex steroid hormones* [Master's thesis]. Norwegian University of Science and Technology. https://hdl.handle.net/11250/3013358

Gebbink, W. A., & Letcher, R. J. (2012). Comparative tissue and body compartment accumulation and maternal transfer to eggs of perfluoroalkyl sulfonates and carboxylates in Great Lakes herring gulls. *Environmental Pollution*, *162*, 40–47. https://doi.org/10.1016/j.envpol.2011.10.011

Geng, D., Musse, A. A., Wigh, V., Carlsson, C., Engwall, M., Orešič, M., Scherbak, N., & Hyötyläinen, T. (2019). Effect of perfluorooctanesulfonic acid (PFOS) on the liver lipid metabolism of the developing chicken embryo. *Ecotoxicology and Environmental Safety*, *170*, 691–698. https://doi.org/10.1016/j.ecoenv.2018.12.040

Griffiths-Jones, S., Grocock, R. J., Van Dongen, S., Bateman, A., & Enright, A. J. (2006). miRBase: MicroRNA sequences, targets and gene nomenclature. *Nucleic Acids Research*, *34*, D140–D144. https://doi.org/10.1093/nar/gkj112

Gu, L., Xu, T., Huang, W., Xie, M., Sun, S., & Hou, S. (2014). Identification and profiling of microRNAs in the embryonic breast muscle of pekin duck. *PloS One*, *9*, e86150. https://doi.org/10.1371/journal.pone.0086150

Gui, W., Guo, H., Chen, X., Wang, J., Guo, Y., Zhang, H., Zhou, X., Zhao, Y., & Dai, J. (2023). Emerging polyfluorinated compound Nafion by-product 2 disturbs intestinal homeostasis in zebrafish (*Danio rerio*). *Ecotoxicology and Environmental Safety*, *249*, 114368. https://doi.org/10.1016/j.ecoenv.2022.114368

Guo, Y., Yuan, J., Ni, H., Ji, J., Zhong, S., Zheng, Y., & Jiang, Q. (2022). Perfluorooctanoic acid-induced developmental cardiotoxicity in chicken embryo: Roles of miR-490-5p. *Environmental Pollution*, *312*, 120022. https://doi.org/10.1016/j.envpol.2022.120022

Heikkila, J. J. (2017). The expression and function of hsp30-like small heat shock protein genes in amphibians, birds, fish, and reptiles. *Comparative Biochemistry and Physiology. Part A, Molecular & Integrative Physiology*, *203*, 179–192. https://doi.org/10.1016/j.cbpa.2016.09.011

Houde, M., Douville, M., Despatie, S.-P., De Silva, A. O., & Spencer, C. (2013). Induction of gene responses in St Lawrence River northern pike (*Esox lucius*) environmentally exposed to perfluorinated compounds. *Chemosphere*, *92*, 1195–1200. https://doi.org/10.1016/j.chemosphere.2013.01.099

Houde, M., Douville, M., Giraudo, M., Jean, K., Lépine, M., Spencer, C., & De Silva, A. O. (2016). Endocrine-disruption potential of perfluoroethylcyclohexane sulfonate (PFECHS) in chronically exposed *Daphnia magna*. *Environmental Pollution*, *218*, 950–956. https://doi.org/10.1016/j.envpol.2016.08.043

Hua, K., Li, Y., Chen, H., Ni, J., Bi, D., Luo, R., & Jin, H. (2018). Functional characterization of duck TBK1 in IFN-β induction. *Cytokine*, *111*, 325–333. https://doi.org/10.1016/j.cyto.2018.09.007

John, B., Enright, A. J., Aravin, A., Tuschl, T., Sander, C., & Marks, D. S. (2004). Human microRNA targets. *PLoS Biology*, *2*, e363. https://doi.org/10.1371/journal.pbio.0020363

Judson, R., Houck, K., Martin, M., Richard, A. M., Knudsen, T. B., Shah, I., Little, S., Wambaugh, J., Woodrow Setzer, R., Kothiya, P., Phuong, J., Filer, D., Smith, D., Reif, D., Rotroff, D., Kleinstreuer, N., Sipes, N., Xia, M., Huang, R., … Thomas, R. S. (2016). Editor's highlight: Analysis of the effects of cell stress and cytotoxicity on *in vitro* assay activity across a diverse chemical and assay space. *Toxicological Sciences: An Official Journal of the Society of Toxicology*, *152*, 323–339. https://doi.org/10.1093/toxsci/kfw092

Kang, W., Eldfjell, Y., Fromm, B., Estivill, X., Biryukova, I., & Friedländer, M. R. (2018). miRTrace reveals the organismal origins of microRNA sequencing data. *Genome Biology*, *19*, 213–215. https://doi.org/10.1186/s13059-018-1588-9

Kertesz, M., Iovino, N., Unnerstall, U., Gaul, U., & Segal, E. (2007). The role of site accessibility in microRNA target recognition. *Nature Genetics*, *39*, 1278–1284. https://doi.org/10.1038/ng2135

Kolberg, L., Raudvere, U., Kuzmin, I., Adler, P., Vilo, J., & Peterson, H. (2023). g:Profiler—interoperable web service for functional enrichment analysis and gene identifier mapping (2023 update). *Nucleic Acids Research*, *51*, W207–W212. https://doi.org/10.1093/nar/gkad347

Kozomara, A., Birgaoanu, M., & Griffiths-Jones, S. (2019). miRBase: From microRNA sequences to function. *Nucleic Acids Research*, *47*, D155–D162. https://doi.org/10.1093/nar/gky1141

Kozomara, A., & Griffiths-Jones, S. (2014). miRBase: Annotating high confidence microRNAs using deep sequencing data. *Nucleic Acids Research*, *42*, D68–D73. https://doi.org/10.1093/nar/gkt1181

Krichevsky, A. M., & Gabriely, G. (2009). miR-21: A small multi-faceted RNA. *Journal of Cellular and Molecular Medicine*, *13*, 39–53. https://doi.org/10.1111/j.1582-4934.2008.00556.x

Kwiatkowski, C. F., Andrews, D. Q., Birnbaum, L. S., Bruton, T. A., DeWitt, J. C., Knappe, D. R. U., Maffini, M. V., Miller, M. F., Pelch, K. E., Reade, A., Soehl, A., Trier, X., Venier, M., Wagner, C. C., Wang, Z., & Blum, A. (2020). Scientific basis for managing PFAS as a chemical class. *Environmental Science & Technology Letters*, *7*, 532–543. https://doi.org/10.1021/acs.estlett.0c00255

Langmead, B., Trapnell, C., Pop, M., & Salzberg, S. L. (2009). Ultrafast and memory-efficient alignment of short DNA sequences to the human genome. *Genome Biology*, *10*, R25–R10. https://doi.org/10.1186/gb-2009-10-3-r25

Liao, Y., Smyth, G. K., & Shi, W. (2014). featureCounts: An efficient general purpose program for assigning sequence reads to genomic features. *Bioinformatics*, *30*, 923–930. https://doi.org/10.1093/bioinformatics/btt656

Liu, Y., Chen, L., Yu, J., Ye, L., Hu, H., Wang, J., & Wu, B. (2022). Advances in single-cell toxicogenomics in environmental toxicology. *Environmental Science & Technology*, *56*, 11132–11145. https://doi.org/10.1021/acs.est.2c01098

Lloyd, D. J., Bohan, S., & Gekakis, N. (2006). Obesity, hyperphagia and increased metabolic efficiency in Pc1 mutant mice. *Human Molecular Genetics*, *15*, 1884–1893. https://doi.org/10.1093/hmg/ddl111

Love, M. I., Huber, W., & Anders, S. (2014). Moderated estimation of fold change and dispersion for RNA-seq data with DESeq2.

Genome Biology, 15, 550–521. https://doi.org/10.1186/s13059-014-0550-8

Magor, K. E., Navarro, D. M., Barber, M. R., Petkau, K., Fleming-Canepa, X., Blyth, G. A., & Blaine, A. H. (2013). Defense genes missing from the flight division. *Developmental and Comparative Immunology*, 41, 377–388. https://doi.org/10.1016/j.dci.2013.04.010

Mahoney, H., Ankley, P., Roberts, C., Lamb, A., Schultz, M., Zhou, Y., Giesy, J. P., & Brinkmann, M. (2024). Unveiling the molecular effects of replacement and legacy PFASs: Transcriptomic analysis of zebrafish embryos reveals surprising similarities and potencies. *Environmental Science & Technology*, 58, 18554–18565. https://doi.org/10.1021/acs.est.4c04246

Mahoney, H., Cantin, J., Rybchuk, J., Xie, Y., Giesy, J. P., & Brinkmann, M. (2023a). Acute exposure of zebrafish (*Danio rerio*) to the next-generation perfluoroalkyl substance, perfluoroethylcyclohexanesulfonate, shows similar effects as legacy substances. *Environmental Science & Technology*, 57, 4199–4207. https://doi.org/10.1021/acs.est.2c08463

Mahoney, H., Cantin, J., Xie, Y., Brinkmann, M., & Giesy, J. P. (2023b). Perfluoroethylcyclohexane sulphonate, an emerging perfluoroalkyl substance, disrupts mitochondrial membranes and the expression of key molecular targets *in vitro*. *Aquatic Toxicology*, 257, 106453. https://doi.org/10.1016/j.aquatox.2023.106453

Mandour, D. A., Morsy, M. M., Fawzy, A., Mohamed, N. M., & Ahmad, M. M. (2023). Structural and molecular changes in the rat myocardium following perfluoroctane sulfonate (PFOS) exposure are mitigated by quercetin via modulating HSP 70 and SERCA 2. *Journal of Molecular Histology*, 54, 283–296. https://doi.org/10.1007/s10735-023-10134-9

Mattsson, A., Sjöberg, S., Kärrman, A., & Brunström, B. (2019). Developmental exposure to a mixture of perfluoroalkyl acids (PFAAs) affects the thyroid hormone system and the bursa of Fabricius in the chicken. *Scientific Reports*, 9, 19808. https://doi.org/10.1038/s41598-019-56200-9

Matz, M. V., Wright, R. M., & Scott, J. G. (2013). No control genes required: Bayesian analysis of qRT-PCR data. *PloS One*, 8, e71448. https://doi.org/10.1371/journal.pone.0071448

McGeary, S. E., Lin, K. S., Shi, C. Y., Pham, T. M., Bisaria, N., Kelley, G. M., & Bartel, D. P. (2019). The biochemical basis of microRNA targeting efficacy. *Science*, 366, eaav1741. https://doi.org/10.1126/science.aav1741

Niu, Z., Na, J., Xu, W., Wu, N., & Zhang, Y. (2019). The effect of environmentally relevant emerging per-and polyfluoroalkyl substances on the growth and antioxidant response in marine *Chlorella* sp. *Environmental Pollution*, 252, 103–109. https://doi.org/10.1016/j.envpol.2019.05.103

Noble, R., & Cocchi, M. (1990). Lipid metabolism and the neonatal chicken. *Progress in Lipid Research*, 29, 107–140. https://doi.org/10.1016/0163-7827(90)90014-c

Ojo, A. F., Peng, C., & Ng, J. C. (2021). Assessing the human health risks of per-and polyfluoroalkyl substances: A need for greater focus on their interactions as mixtures. *Journal of Hazardous Materials*, 407, 124863. https://doi.org/10.1016/j.jhazmat.2020.124863

Peterson, S. (2024). *Developmental effects and endocrine disrupting potential of in ovo exposure to per- and polyfluoroalkyl substances (PFASs) in mallard ducklings (Anas platyrhynchos)* [Master's thesis]. Norwegian University of Science and Technology. https://ntnuopen.ntnu.no/ntnu-xmlui/handle/

Pfaffl, M. W., Tichopad, A., Prgomet, C., & Neuvians, T. P. (2004). Determination of stable housekeeping genes, differentially regulated target genes and sample integrity: BestKeeper–Excel-based tool using pair-wise correlations. *Biotechnology Letters*, 26, 509–515. https://doi.org/10.1023/b: bile.0000019559.84305.47

R Core Team (2023). A language and environment for statistical computing. Foundation for Statistical Computing.

Rajak, P., & Ganguly, A. (2023). The ligand-docking approach explores the binding affinity of PFOS and PFOA for major endogenous antioxidants: A potential mechanism to fuel oxidative stress. *Sustainable Chemistry for the Environment*, 4, 100047. https://doi.org/10.1016/j.scenv.2023.100047

Robuck, A. R., McCord, J. P., Strynar, M. J., Cantwell, M. G., Wiley, D. N., & Lohmann, R. (2021). Tissue-specific distribution of legacy and novel per-and polyfluoroalkyl substances in juvenile seabirds. *Environmental Science & Technology Letters*, 8, 457–462. https://doi.org/10.1021/acs.estlett.1c00222

Roscales, J. L., Vicente, A., Ryan, P. G., Gonzalez-Solis, J., & Jimenez, B. (2019). Spatial and interspecies heterogeneity in concentrations of perfluoroalkyl substances (PFASs) in seabirds of the Southern Ocean. *Environmental Science & Technology*, 53, 9855–9865. https://doi.org/10.1021/acs.est.9b02677

Rueda, A., Barturen, G., Lebrón, R., Gómez-Martín, C., Alganza, Á., Oliver, J. L., & Hackenberg, M. (2015). sRNAtoolbox: An integrated collection of small RNA research tools. *Nucleic Acids Research*, 43, W467–W473. https://doi.org/10.1093/nar/gkv555

Schat, K. A., Kaspers, B., & Kaiser, P. (2014). *Avian immunology*. Elsevier.

Seremelis, I., Danezis, G. P., Pappas, A. C., Zoidis, E., & Fegeros, K. (2019). Avian stress-related transcriptome and selenotranscriptome: Role during exposure to heavy metals and heat stress. *Antioxidants*, 8, 216. https://doi.org/10.3390/antiox8070216

Seth, R. B., Sun, L., Ea, C.-K., & Chen, Z. J. (2005). Identification and characterization of MAVS, a mitochondrial antiviral signaling protein that activates NF-κB and IRF3. *Cell*, 122, 669–682. https://doi.org/10.1016/j.cell.2005.08.012

Shepherd, R., Cheung, A. S., Pang, K., Saffery, R., & Novakovic, B. (2020). Sexual dimorphism in innate immunity: The role of sex hormones and epigenetics. *Frontiers in Immunology*, 11, 604000. https://doi.org/10.3389/fimmu.2020.604000

Singam, E. R. A., Durkin, K. A., La Merrill, M. A., Furlow, J. D., Wang, J.-C., & Smith, M. T. (2023). The vitamin D receptor as a potential target for the toxic effects of per-and polyfluoroalkyl substances (PFASs): An in-silico study. *Environmental Research*, 217, 114832. https://doi.org/10.1016/j.envres.2022.114832

Snell, T. W., Brogdon, S. E., & Morgan, M. B. (2003). Gene expression profiling in ecotoxicology. *Ecotoxicology*, 12, 475–483. https://doi.org/10.1023/b: ectx.0000003033.09923.a8

Spalluto, C. M., Singhania, A., Cellura, D., Woelk, C. H., Sanchez-Elsner, T., Staples, K. J., & Wilkinson, T. M. (2017). IFN-γ influences epithelial antiviral responses via histone methylation of the RIG-I promoter. *American Journal of Respiratory Cell and Molecular Biology*, 57, 428–438. https://doi.org/10.1165/rcmb.2016-0392OC

Staeva-Vieira, T. P., & Freedman, L. P. (2002). 1, 25-dihydroxyvitamin D3 inhibits IFN-γ and IL-4 levels during *in vitro* polarization of primary murine CD4+ T cells. *Journal of Immunology*, 168, 1181–1189. https://doi.org/10.4049/jimmunol.168.3.1181

Stijnen, P., Ramos-Molina, B., O'Rahilly, S., & Creemers, J. W. (2016). PCSK1 mutations and human endocrinopathies: From obesity to gastrointestinal disorders. *Endocrine Reviews*, 37, 347–371. https://doi.org/10.1210/er.2015-1117

Sturm, M., Hackenberg, M., Langenberger, D., & Frishman, D. (2010). TargetSpy: A supervised machine learning approach for microRNA target prediction. *BMC Bioinformatics*, 11, 292–217. https://doi.org/10.1186/1471-2105-11-292

Sun, J., Xing, L., & Chu, J. (2023). Global ocean contamination of per-and polyfluoroalkyl substances: A review of seabird exposure. *Chemosphere*, 330, 138721. https://doi.org/10.1016/j.chemosphere.2023.138721

Surina, S., Fontanella, R. A., Scisciola, L., Marfella, R., Paolisso, G., & Barbieri, M. (2021). miR-21 in human cardiomyopathies. *Frontiers in Cardiovascular Medicine*, *8*, 767064. https://doi.org/10.3389/fcvm.2021.767064

Tian, M., Peng, S., Martin, F. L., Zhang, J., Liu, L., Wang, Z., Dong, S., & Shen, H. (2012). Perfluorooctanoic acid induces gene promoter hypermethylation of glutathione-S-transferase Pi in human liver L02 cells. *Toxicology*, *296*, 48–55. https://doi.org/10.1016/j.tox.2012.03.003

Untergasser, A., Ruijter, J. M., Benes, V., & van den Hoff, M. J. (2021). Web-based LinRegPCR: Application for the visualization and analysis of (RT)-qPCR amplification and melting data. *BMC Bioinformatics*, *22*, 398. https://doi.org/10.1186/s12859-021-04306-1

Vandesompele, J., De Preter, K., Pattyn, F., Poppe, B., Van Roy, N., De Paepe, A., & Speleman, F. (2002). Accurate normalization of real-time quantitative RT-PCR data by geometric averaging of multiple internal control genes. *Genome Biology*, *3*, RESEARCH0034–12. https://doi.org/10.1186/gb-2002-3-7-research0034

Vychytilova-Faltejskova, P., & Slaby, O. (2019). MicroRNA-215: From biology to theranostic applications. *Molecular Aspects of Medicine*, *70*, 72–89. https://doi.org/10.1016/j.mam.2019.03.002

Wang, J., Yan, S., Zhang, W., Zhang, H., & Dai, J. (2015). Integrated proteomic and miRNA transcriptional analysis reveals the hepatotoxicity mechanism of PFNA exposure in mice. *Journal of Proteome Research*, *14*, 330–341. https://doi.org/10.1021/pr500641b

Wang, L., Li, X., Ma, J., Zhang, Y., & Zhang, H. (2017). Integrating genome and transcriptome profiling for elucidating the mechanism of muscle growth and lipid deposition in Pekin ducks. *Scientific Reports*, *7*, 3837. https://doi.org/10.1038/s41598-017-04178-7

Wen, Z.-J., Wei, Y.-J., Zhang, Y.-F., & Zhang, Y.-F. (2023). A review of cardiovascular effects and underlying mechanisms of legacy and emerging per-and polyfluoroalkyl substances (PFAS). *Archives of Toxicology*, *97*, 1195–1245. https://doi.org/10.1007/s00204-023-03477-5

Wetlands International (2025). *Waterbird populations portal*. Wetlands International. https://wpp.wetlands.org/

Wickham, H. (2011). ggplot2. *WIREs Computational Statistics*, *3*, 180–185. https://doi.org/10.1002/wics.147

Wystub, K., Besser, J., Bachmann, A., Boettger, T., & Braun, T. (2013). miR-1/133a clusters cooperatively specify the cardiomyogenic lineage by adjustment of myocardin levels during embryonic heart development. *PLoS Genetics*, *9*, e1003793. https://doi.org/10.1371/journal.pgen.1003793

Xu, X., Zhang, X., Chen, J., Du, X., Sun, Y., Zhan, L., Wang, W., & Li, Y. (2024). Exploring the molecular mechanisms by which per-and polyfluoroalkyl substances induce polycystic ovary syndrome through *in silico* toxicogenomic data mining. *Ecotoxicology and Environmental Safety*, *275*, 116251. https://doi.org/10.1016/j.ecoenv.2024.116251

Yang, H., Wang, Y., Liu, M., Liu, X., Jiao, Y., Jin, S., Shan, A., & Feng, X. (2021). Effects of dietary resveratrol supplementation on growth performance and anti-inflammatory ability in ducks (*Anas platyrhynchos*) through the Nrf2/HO-1 and TLR4/NF-κB signaling pathways. *Animals: An Open Access Journal from MDPI*, *11*, 3588. https://doi.org/10.3390/ani11123588

Yao, D., Shao, J., Jia, D., & Sun, W. (2024). Immunotoxicity of legacy and alternative per-and polyfluoroalkyl substances on zebrafish larvae. *Environmental Pollution*, *358*, 124511. https://doi.org/10.1016/j.envpol.2024.124511

Ye, J., Coulouris, G., Zaretskaya, I., Cutcutache, I., Rozen, S., & Madden, T. L. (2012). Primer-BLAST: A tool to design target-specific primers for polymerase chain reaction. *BMC Bioinformatics*, *13*, 134–111. https://doi.org/10.1186/1471-2105-13-134

Zhang, W.-X., Zuo, E.-W., He, Y., Chen, D.-Y., Long, X., Chen, M.-J., Li, T.-T., Yang, X.-G., Xu, H.-Y., Lu, S.-S., Zhang, M., Lu, K.-H., & Lu, Y.-Q. (2016). Promoter structures and differential responses to viral and non-viral inducers of chicken melanoma differentiation-associated gene 5. *Molecular Immunology*, *76*, 1–6. https://doi.org/10.1016/j.molimm.2016.06.006

Zhang, Y., Chen, Y., Gu, T., Xu, Q., Zhu, G., & Chen, G. (2019). Effects of *Salmonella enterica* serovar Enteritidis infection on egg production and the immune response of the laying duck *Anas platyrhynchos*. *PeerJ*, *7*, e6359. https://doi.org/10.7717/peerj.6359

Environmental Toxicology and Chemistry, 2025, 00, 1–15
https://doi.org/10.1093/etojnl/vgaf213
Original Article